Korean J. Chem. Eng., **31**(5), 821-827 (2014)
DOI: 10.1007/s11814-014-0004-8

pISSN: 0256-1115
eISSN: 1975-7220

Preparation and adsorption characters of Cu(II)-imprinted chitosan/attapulgite polymer

Yingying Shi†, Qianghua Zhang, Liangdong Feng, Qingping Xiong, and Jing Chen

Department of Chemical Engineering, Huaiyin Institute of Technology,
Key Laboratory for Palygorskite Science and Applied Technology of Jiangsu Province, Jiangsu Huai'an 223003, China
(*Received 17 August 2013 • accepted 4 January 2014*)

Abstract−Using attapulgite (ATP) as matrix, chitosan (CS) as functional monomer, and introducing the surface ion-imprinting concept, a new Cu(II)-IIP was prepared, and characterized by SEM, XRD and FT-IR. The adsorption of Cu(II) aqueous solution with Cu(II)-IIP was investigated by flame atomic adsorption spectroscopy (FAAS). The polymer has good selectivity for Cu(II) from competitive metal ions, and the selectivity coefficient of Cu(II) relation to Pb(II), Cd(II) was 78.45 and 82.44, respectively. Sorption equilibrium isotherms could be described by Langmuir and Freundlich models; the Freundlich isotherm has shown the best agreement with experimental data, and experimental value of maximum adsorption capacity for Cu(II) was 35.20 mg/g. The obtained thermodynamic parameter (ΔG^o, ΔH^o, ΔS^o) showed that the Cu(II) adsorption process is a spontaneous and endothermic process. The kinetic data showed that pseudo-second-order kinetic model agrees very well with the dynamic behavior for the sorption of Cu(II) onto Cu(II)-IIP.

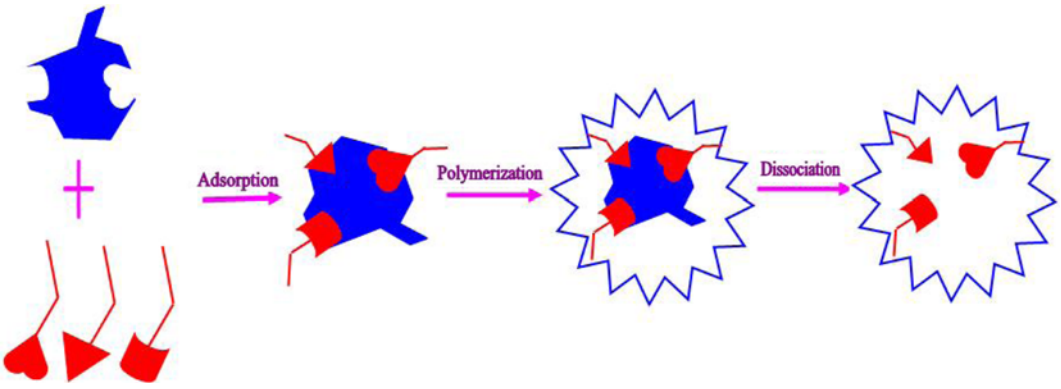

Keywords: Attapulgite, Chitosan (CS), Ion-imprinting, Adsorption Isotherms, Selective Recognition, Cu(II)

INTRODUCTION

Toxic heavy metal ions are discharged into the environment by various industrial activities such as fertilizer industries, refining ores, mining, tanneries, batteries, pesticides, paper industries etc. [1], causing serious water and soil pollution. Stringent regulations have increased the demand for new technologies for metal removal from waste water to obtain present toxicity driven limits [2]. Heavy metals are not easily biodegradable and are easily accumulated by live organisms, causing various diseases and disorders [3]. Cu(II) is one of the most toxic heavy metals found in industrial wastewater. Its toxic and persistent characteristics cause concern when effluents containing Cu(II) are discharged to receiving water bodies without proper treatment. The Cu(II) can accumulate along the food chain, finally linked to human health problems.

Methods such as chemical precipitation, electrochemical treatment, membrane filtration, solvent extraction, ion exchange, adsorption, etc. [4] have been used to deal with the metal wastewater. Adsorption is a process of removing molecules or ions from the surrounding media onto the surface of solid material by sorption. It has more advantages including recovery capability of metal, selectivity, and cost effectiveness [5]. Many adsorbents have been used to remove heavy metals such as sawdust [6,7], activated phosphate [8], activated carbon [9,10], etc. Among these, activated carbon has been successfully applied for heavy metal removal. But, the use is hampered by its high cost [11]. In recent years, low cost adsorbents developed from kinds of materials [12-16] have gained attention because their double benefit of resource regeneration and pollution abatement.

Recently, many researchers have focused on a new kind of non-metallic mineral material, attapulgite clay[$Si_8O_{20}Mg_5(Al)(OH)_2(H_2O)_4 \cdot 4H_2O$]. Attapulgite consists of double silica tetrahedral chains linked together by octahedral oxygen and hydroxyl groups containing Al and Mg ions in a chain-like inverted structure, and it has large surface area, porous structure and appropriate cation exchange capacity. Attapulgite has been intensively used as adsorbent in the removing process of heavy metal ions and organic contaminants such as lead, cadmium, copper, uranium and thorium ions [17-21]. But it is necessary to enhance its adsorption capacity and selective recognition.

CS, a part of deacetylated product of chitin, has a number of useful

†To whom correspondence should be addressed.
E-mail: shiyingying82012@gmail.com
Copyright by The Korean Institute of Chemical Engineers.

Table 1. Working conditions of FAAS

Lamp current (mA)	Narrow aperture (nm)	Wavelength (nm)	Negative high-voltage (V)	Acetylene flow rate (L/min)	Burner position (mm)	Burner height (mm)
6.0	0.4	324.8	311.0	1.5	0.2	5

features such as biodegradability, biocompatibility, antibacterial property and high resistance to heat because of intramolecular hydrogen bonds formed between amino (-NH_2) and hydroxyl (-OH). Amine and hydroxyl groups in CS could be available for characteristic coordination bonding with metal ions such as lead, cadmium, copper, zinc and uranium ions [22-27]. But, CS is just soluble in little dilute acid solutions, and it has defects of swelling and dissatisfying mechanical property.

Ion-imprinting is a powerful method to synthesis ion-imprinted polymer (IIP). The preparation of IIPs based on the ion-imprinting concept is described as follows: a matrix is synthesized in the presence of an ionic template, and chelating resins are then obtained by removal of the targeted ion. The cavities left obtained in the polymer exhibit high selectivity towards specific metal ions [28-33]. More and more attention has been paid to the research of the surface-imprinting technique, based on support materials (i.e., TiO_2, SiO_2, α-Al_2O_3, CdS, magnetic Fe_3O_4, etc.), which offers faster mass transfer kinetics. Attapulgite has the possibility to act as an inorganic support material in the preparation of surface-imprinted polymer because of its particular intensity, special structure, stable chemical properties and abundant raw materials.

The purpose of the present study is to use attapulgite as matrix, and apply the surface ion-imprinting concept and CS incorporated sol-gel process to the preparation of a new attapulgite-supported organic-inorganic hybrid polymer for selective separation of Cu(II) from aqueous solution. The materials were characterized by SEM, XRD and FT-IR. The adsorption behavior, adsorption kinetics, adsorption isotherms, and thermodynamics of Cu(II) adsorption onto the composite were studied.

EXPERIMENTAL

1. Materials and Chemicals

Attapulgite clay was provided by Mingguang Xiqi Co., (Anhui, China). It was decentralized in 3.0 mol/L HCl and soaked for 12 h at room temperature. Then, the material was washed with water until neutral pH of solution, dried in vacuum at 40 ºC for 24 h. In the end, it was ground, sifted with 100 meshes. Chitosa with 90% de-acetylating degree, ethylene glycol dimethacrylate (EGDMA), azodiisobutyronitrile (ABN) were purchased from Sigma-Aldrich (St. Louis, MO, USA). Acetic acid, oxalic acid, hydrochloric acid, sodium hydroxide, copper(II) sulfate were purchased from Sinopharm Chemical Reagent Co., Ltd. (Shanghai, China). Experimental water all for doubly distilled water (DDW), was made by ourselves.

2. Instrumentation

Scanning electron microscopy (SEM) images were obtained at 5.0 kV on the field emission scanning electron microscope (Hitachi Limited, Japan) after gold plating. D8 Discover X-ray diffraction (XRD) (Bruker, Germany). Nicolet 5700 FT-IR (Thermo Electron Co., USA). TAS-990 flame atomic adsorption spectrometer (FAAS) (Beijing Purkinje General Instrument Co., Beijing, China). The main operating conditions are shown in Table 1. STA 409 (Netzsch Inc., Germany). YHG-500-BS Far infrared fast drying oven (Shanghai Botai Experimental Equipments Co., Ltd., Shanghai, China). FA2004N Electronic balance (Shanghai Sunny Hengping Scientific Instrument Co., Ltd., Shanghai, China). Model PHS-25 pH Meter (Shanghai Shengci Co., Shanghai, China).

3. Preparation of Ion-imprinted Composite Sorbent

The composites of Cu(II)-IIP was prepared as follows: 10.0 g CS was dissolved in a mixture of 20 mL of oxalic acid-water (1 : 10, w/w) and 5 mL of acetic acid-water (1 : 100, w/w). 15.0 g activated attapulgite was added to the solution under stirring for 1 h. Then the solid was filtered and dried under vacuum at 55 ºC to constant weight; this resulting product was chitosan/attapulgite (CA). Dissolving the above materials with DDW, a certain amount of copper(II) sulfate was added to the solution under stirring for 4 h. Then 60.0 g EGDMA and ABN was added to the transparent solution, respectively. The water was evaporated at room temperature to complete the cross-linking reaction and gelation. The consequent Cu(II)-complexed composite was filtered and washed by 0.1 mol/L HCl solution until the Cu(II) concentration in the washings was undetectable by FASS. The resulting gels were neutralized with 0.1 mol/L NaOH to pH 7, filtered, washed several times with DDW, and dried under vacuum at 50 ºC for 12 h. By comparison, the non-imprinted polymer (non-IIP) was also prepared as a blank in parallel but without the addition of Cu(II).

4. Investigation of the Structural Characteristics

The raw attapulgite, non-IIP and Cu(II)-IIP were analyzed by using an SEM to study the surface morphology at the desired magnification. These three samples were analyzed by XRD at a scanning rate of 4º/min in the 2θ range from 5 to 70º, with graphite monochromatized Cu Kα radiation (λ=0.15418 nm) and nickel filter to study the crystal structures. FT-IR (4,000 to 400 cm^{-1}) with KBr pellets and a resolution of 1 cm^{-1} was recorded under ambient conditions.

5. Adsorption Test

The static adsorption test was carried out in batch experiments. For the effect of pH on the adsorption capacity, 100 mg ion-imprinted composite sorbent was introduced into 100 mL of 40 mg/L Cu(II) solution in the pH from 1.0 to 6.0. For kinetic studies, 100 mg ion-imprinted composite sorbent was introduced into 100 mL of 40 mg/L Cu(II) solution by varying adsorption time in the range of 0-90 min. All experiments were carried out in 250 mL flasks and performed on a thermostatted shaker with a shaking of 180 rpm; the temperature was controlled during each experiment to be within 0.1 ºC. At predetermined times, the samples were withdrawn from the shaker, and the Cu(II) solution was separated from the adsorbent by centrifuging at 4,000 rpm for 15 min. Then, the liquid phase was determined directly by FAAS. Cu(II) concentration was calculated from the calibration curve. The thermodynamic study was performed by varying temperature from (25 to 45) ºC using 1 g/L ion-imprinted composite sorbent added to 50 mL of aqueous Cu(II) solu-

tions in 250 mL flasks. The flasks were shaken at 180 rpm for 100 min. The adsorption capacity (Q_e) was calculated according to Eq. (1).

$$Q_e=(C_o-C_e)V/W \quad (1)$$

where C_o and C_e represent initial and equilibration concentration (mg/L) of the metal ion respectively. V is the volume of solution (L); W is the mass (g) of the sorbent used.

The pH values of initial solutions were adjusted with dilute HCl or NaOH solution by using a pH Meter, and the final volume was diluted with DDW.

The selectivity adsorption experiments of Pb(II) and Cd(II) with respect to Cu(II) were conducted using Cu(II)-IIP or non-IIP. The Pb(II) and Cd(II) ions were chosen as the competitor species because it has the same charge and also binds well with the amino groups. The Cu(II)-IIP or non-IIP sorbent (100 mg) was added to 100 mL of binary metal mixed aqueous solution containing 40 mg/L Cu(II)/Pb(II) ,Cu(II)/Cd(II) at a pH of 5. After adsorption equilibrium, centrifugation, the concentration of each ion in the liquid phase was measured directly by FAAS. The distribution coefficient K_d of metal ion was calculated according to Eq. (2), and the selective coefficient k of coexist interference ion to Cu(II) was calculated following Eq. (3).

$$K_d=Q_e/C_e \quad (2)$$

$$\kappa=K_d(Cu^{2+})/K_d(B) \quad (3)$$

where B represents coexistng interference ions.

6. Adsorption Thermodynamics

In adsorption processes, values of thermodynamic parameters for the adsorption are the actual indicators for practical application. The free energy change of adsorption (ΔG^o), enthalpy change (ΔH^o), and entropy change (ΔS^o) were evaluated by the following equations:

$$\Delta G^o=\Delta H^o-T\Delta S^o \quad (4)$$

$$\Delta G^o=-RT\ln K_c \quad (5)$$

$$K_c=C_{Ae}/C_e \quad (6)$$

$$\ln K_c=\Delta S^o/R-\Delta H^o/RT \quad (7)$$

where K_c is the equilibrium constant, C_{Ae} and C_e (both in mg/L) are the equilibrium concentrations for solute on the sorbent and in the solution, respectively. R is the universal gas constant (8.314 J/mol·K), and T is absolute temperature (K).

7. Adsorption Kinetics

To understand the adsorption mechanism better, characteristic constants of adsorption were determined at 25 °C and pH 5.0 by using a pseudo-first-order equation and Ho pseudo-second-order equation. The pseudo-first-order and pseudo-second-order kinetics model could be expressed as Eq. (8) and Eq. (9):

$$\log(q_e-q_t)=\log q_e-\frac{k_1 t}{2.303} \quad (8)$$

$$\frac{t}{q_t}=\frac{1}{k_2 q_e^2}+\frac{t}{q_e} \quad (9)$$

where k_1 and k_2 are the first and second order rate constant, respectively, q_e and q_t are the amounts of adsorbed Cu(II) ions on the Cu(II)-IIP surface at equilibrium and at any time t, respectively. From Eq. (9), q_e and k_2 values could be obtained from the intercept and slope of the linear plot of q_t versus $t^{1/2}$. When the contact time approached zero, the initial adsorption rate (k_d, g/mg/min) could be obtained according to Eq. (10):

$$q_t=K_d\sqrt{t} \quad (10)$$

8. Adsorption Isotherm

Adsorption isotherms are important for the description of how molecules or ions of adsorbate interact with adsorbent surface sites. Hence, the adsorption of Cu(II) onto Cu(II)-IIP is determined as a function of equilibrium Cu(II) concentration (C_e) and the corresponding adsorption isotherm at 25, 35 and 45 °C. For interpretation of the adsorption data, the Langmuir and Freundlich models were used. The adsorption capacity of Cu(II)-IIP was compared from the Langmuir and Freundlich parameters acquired from the linearized equilibrium metal concentration versus quantity adsorbed at 25, 35, and 45 °C. The Freundlich equation (Eq. (11)) explains adsorption onto a heterogeneous surface with uniform energy:

$$\log q_e=\lg K_F+\frac{1}{n}\lg C_e \quad (11)$$

where q_e and C_e are the equilibrium concentrations of metal in the adsorbed (mg/g) and liquid phases (mg/L), respectively. K_F and n are the Freundlich constants which are related to adsorption capacity and intensity, respectively.

On the other hand, the Langmuir equation (Eq. (12)) is based on monolayer adsorption on active sites of the adsorbent:

$$\frac{C_e}{q_e}=\frac{1}{q_m}C_e+\frac{1}{q_m K_L} \quad (12)$$

where q_e and C_e are equilibrium concentrations of metal in the adsorbed (mg/g) and liquid phases (mg/L), respectively. q_m and K_L are the Langmuir constants which are related to the adsorption capacity and energy of adsorption, respectively.

RESULTS AND DISCUSSION

1. Characterization

The SEM images of the attapulgite (Fig. 1(a)), non-IIP (Fig. 1(b)) and Cu(II)-IIP (Fig. 1(c)) were exemplified by the electron micrographs, and there were some differences in their surface morphology. The SEM image of the raw attapulgite was a randomly oriented network of densely packed fibers, but non-IIP and Cu(II)-IIP displayed a rough surface containing many cavities, while a significant difference compared with before modified. The results strongly showed that the template imprint of Cu(II) was formed within Cu(II)-IIP. It is important to mention the general role Cu(II) played in the preparation process of Cu(II)-IIP, regarding the difference between the Cu(II)-IIP and non-IIP. After polymerization, assembled with Cu(II) as the pivot, monomers were regularly positioned around the templates by a coordinating bridge. And an imprint with a relative higher fidelity was thus left behind the template removal. As shown in Fig. 1(c), its product was successfully grafted onto the surface of attapulgite. Owing to leaching the coordinated Cu(II), many cavities were left on the surface of Cu(II)-IIP, and the coordination bond was stronger than the hydrogen bond used in Cu(II)-IIP.

The XRD analysis of raw attapulgite (a), non-IIP (b) and Cu(II)-

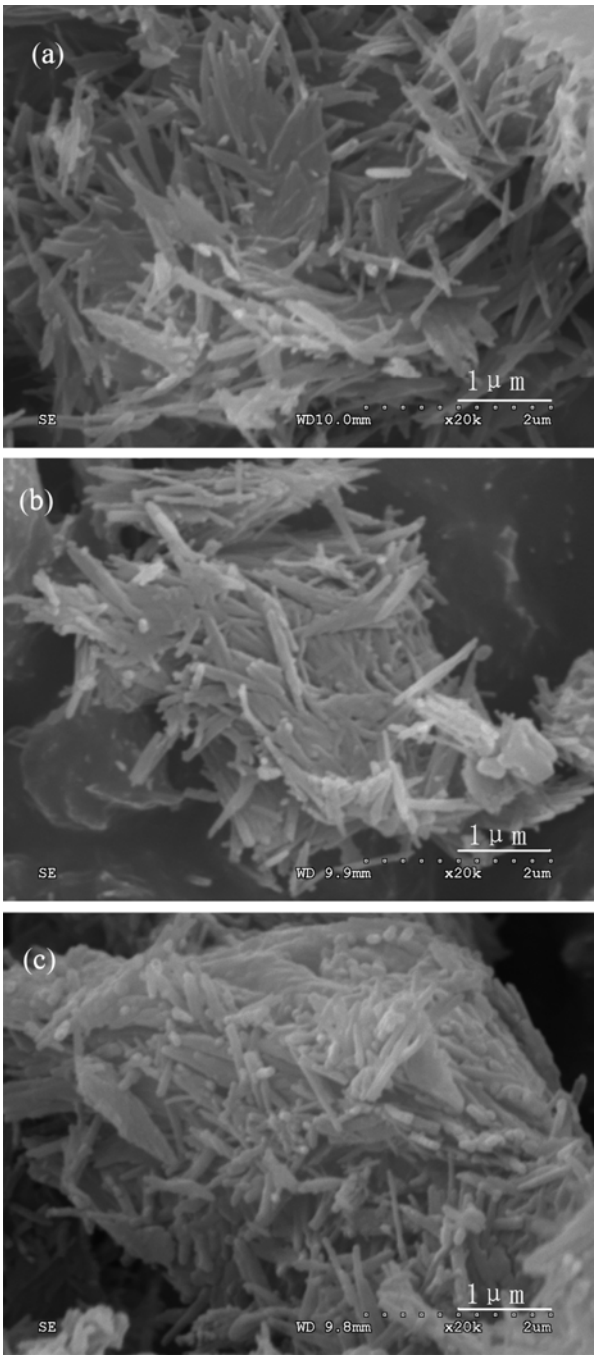

Fig. 1. SEM micrographs of attapulgite (a), Non-IIP (b) and Cu(II)-IIP (c).

IIP (c) is shown in Fig. 2. The crystal structures of non-IIP and Cu(II)-IIP underwent many changes compared with raw attapulgite; the peak positions (2θ=16.3°, 19.8°, and 35.3°) disappeared, and the peak position (2θ=26.7°) weakened. As shown in Fig. 2(c), the cross-linking process between CS coordinated Cu(II) and EGDMA could reduce crystalline domains in the CS and then increase sorption capacity. One peak (2θ=8.34°), which was attributed to the basal plane of attapulgite structure, indicated sharp decrease of crystallization compared with attapulgite. This phenomenon was expected to be available to increase hydrophilicity and enhance metal binding capacity. The results suggested that a new inorganic-organic hybrid material

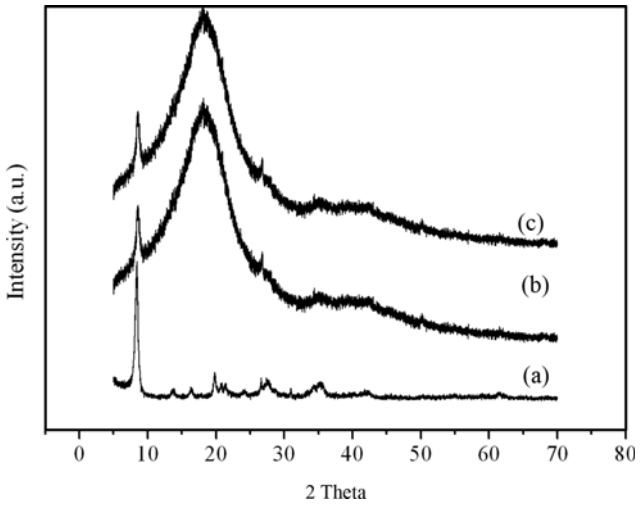

Fig. 2. XRD patterns of attapulgite (a), Non-IIP (b) and Cu(II)-IIP (c).

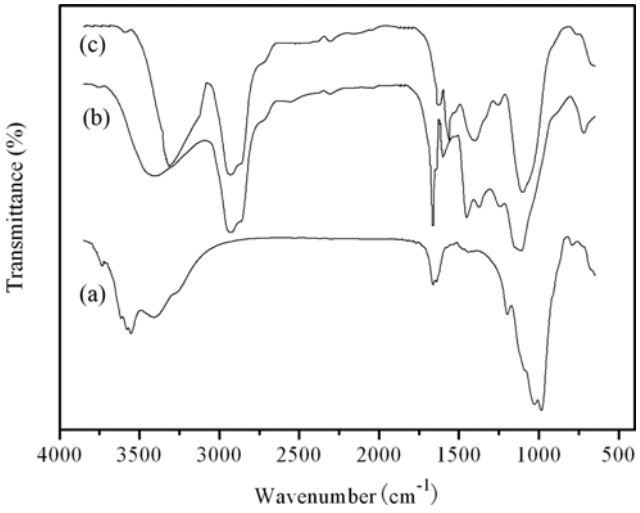

Fig. 3. FT-IR spectra of attapulgite (a), Non-IIP (b) and Cu(II)-IIP (c) films.

was generated.

FT-IR spectra of raw attapulgite (a), non-IIP (b) and Cu(II)-IIP (c) are shown in Fig. 3. The bands around 1,000 cm^{-1}, resulted from Si-O-Si (Al) of attapulgite, changed in the non-IIP and Cu(II)-IIP. Comparing non-IIP with Cu(II)-IIP, a wide and strong peak around 3,402 cm^{-1}, from stretching vibrations of N-H and O-H in CS, shifted to 3,315 cm^{-1} and obviously became narrow in Cu(II)-IIP. Due to the presence of Cu-N bond in the Cu(II)-IIP, the N-H bending vibration of -NH_2 was influenced by the spacial site resistance, and the energy needed by N-H bending vibration increased. This fact resulted in N-H bending vibration bond of -NH_2 around 1,662 cm^{-1} shift to the lower wavenumber of 1,637 cm^{-1}. The observed features around 1,662 cm^{-1} indicated vibrations of N from -NH_3^+ coordinated with Cu(II).

2. Effect of pH Values of Solution

The effect of pH value on sorption of Cu(II) was evaluated at 25 ºC; 100 mg ion-imprinted composite sorbent was introduced into 100 mL of 40 mg/L Cu(II) solution in the pH from 1.0 to 6.0. At

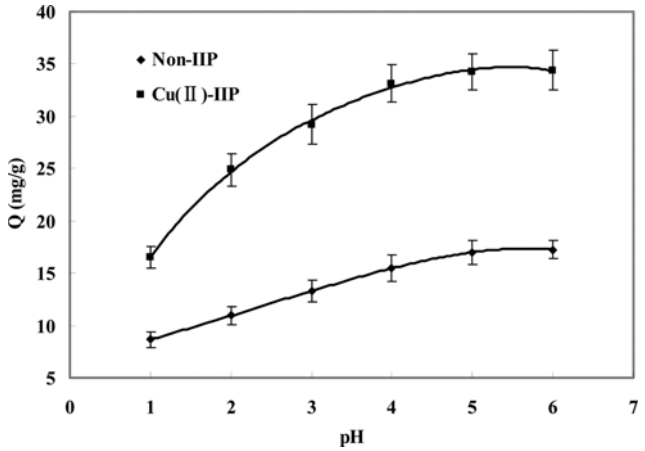

Fig. 4. Effect of pH values on adsorption of Cu(II) on Cu(II)-IIP and Non-IIP.

the same time, the non-IIP materials were studied under the same condition. The pH plays an important role in the whole adsorption process, particularly in the adsorption capacity. The results are shown in Fig. 4. Below pH 1 or so, there is little adsorption of Cu(II), possibly due to the presence of excess H^+ ions competing with Cu(II) ions for the available adsorption sites. The greatest increase in the adsorption capacity is observed for pH changes from 1 to 5, and then small amount of increase of metals is found at pH>6 due to the formation of insoluble hydroxide forms of metals. As the pH increases from 1 to 6, the active sites become increasingly ionized and the Cu(II) ions become adsorbed because of the ion-exchange on the phosphate groups and chelation on the amino groups. The optimum pH for metals adsorption was recorded at pH range of 5-6.

3. Effect of Contact Time

The time-dependent behavior of Cu(II) adsorption was measured at 25 ºC; 100 mg ion-imprinted composite sorbent was introduced into 100 mL of 40 mg/L Cu(II) solution by varying adsorption time in the range of 0-90 min. At the same time, the non-IIP materials were studied under the same condition. The results (Fig. 5) showed rapid adsorption of Cu(II) in the first 40 min. After that, the adsorption rate decreased, and the adsorption equilibrium was achieved in

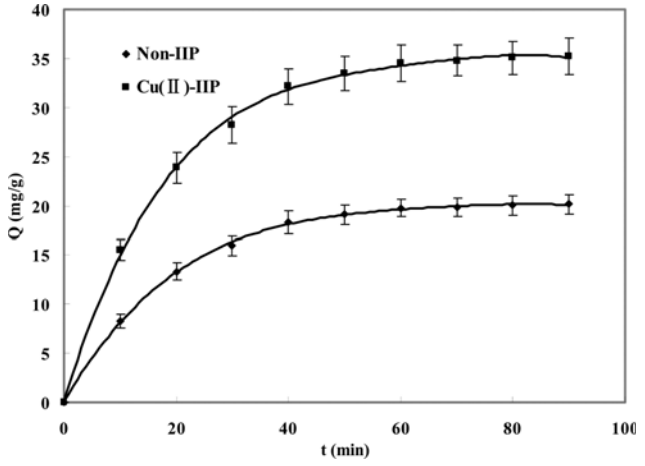

Fig. 5. Effect of time on adsorption of Cu(II) on Cu(II)-IIP and Non-IIP.

Table 2. Values of thermodynamic parameters for Cu(II) sorption

T (K)	ΔG^o (kJ/mol)	ΔS^o (J/mol·K)	ΔH^o (kJ/mol)	R^2
298.15	−0.73	101.12	29.36	0.9864
308.15	−1.87			
318.15	−2.57			

60 min. It explains that the Cu(II)-IIP surface was progressively obstructed by the Cu(II) reaching pseudo-equilibrium in approximately 60 min. In this time, the amount of Cu(II) being adsorbed onto the Cu(II)-IIP is in dynamic equilibrium with the Cu(II) amount desorbed from the adsorbent. The maximum adsorption capacity is found to be 35.20 mg/g.

4. Adsorption Thermodynamics

Based on Eqs. (4)-(7), the enthalpy change ΔH^o (kJ/mol), and entropy change (J/mol·K) were calculated from the slope and intercept of linear plot of $\ln K_c$ versus 1/T, respectively. The thermodynamic parameters ΔG^o, ΔH^o, ΔS^o are shown in Table 2. The ΔH^o and ΔS^o for the adsorption process were calculated to be 26.65 kJ/mol and 92.07 J/mol·K, respectively. The negative values of the free energy (ΔG^o) at the three temperatures confirms that the adsorption process was feasible and spontaneous nature of adsorption with a high preference for Cu(II) onto Cu(II)-IIP. The positive value of the standard enthalpy change (ΔH^o) showed that the adsorption reaction is endothermic, because Cu(II) is dissolved well in water, and that the hydration sheath of Cu(II) has to be destroyed before its

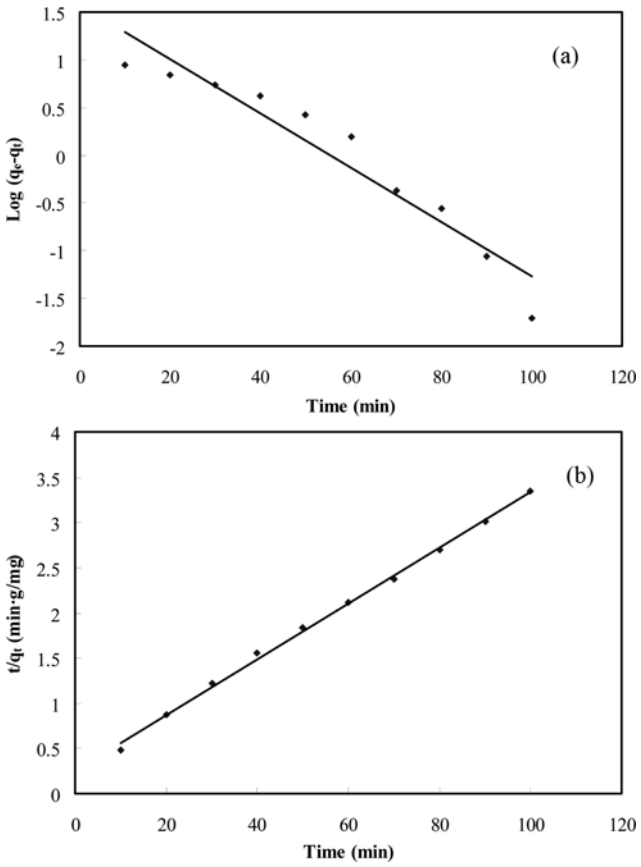

Fig. 6. Pseudo-first-order (a) and pseudo-second-order (b) for the adsorption of Cu(II) on Cu(II)-IIP at 25 ºC.

Table 3. Kinetic parameters of pseudo-first-order and pseudo-second-order model

Pseudo-first-order model			Pseudo-second-order model		
q_e (mg/g)	k_1 (g/mg·min)	R^2	q_e (mg/g)	k_1 (g/mg·min)	R^2
47.24	0.0654	0.9200	32.36	0.0038	0.9978

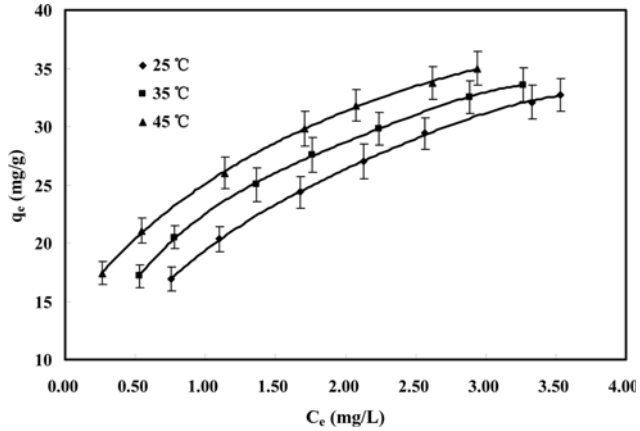

Fig. 7. Adsorption isothermal curves on Cu(II)-IIP at 25, 35 and 45 °C for Cu(II).

adsorption on Cu(II)-IIP. This dehydration process needs energy, so it is favored at high temperature. The positive value of entropy change (ΔS^o) suggested a degree of randomness or disorder at the solid/liquid interface during the adsorption of Cu(II) ions onto Cu(II)-IIP.

5. Adsorption Kinetics

The graphical presentations for pseudo-first-order and pseudo-second-order kinetics model are given in Fig. 6. All of the parameters mentioned above were determined as shown in Table 3. The obtained correlation coefficients indicated that both pseudo-first-order and pseudo-second-order model could describe these kinetic parameters. The correlation coefficients for the pseudo-first-order kinetic model was lower, and the results of pseudo-second-order kinetics showed that the linear fit with extremely high correlation coefficients (R^2>0.99) to be close to 1. Moreover, the calculated q_e values were in good agreement with the experimental data. These results show that the rates of adsorption conform to pseudo-second-order kinetics.

6. Adsorption Isotherm

The adsorption of Cu(II) onto Cu(II)-IIP is determined as a function of equilibrium Cu(II) concentration (C_e), and the corresponding adsorption isotherm is plotted in Fig. 7. The equilibrium isotherm for the adsorption of Cu(II) on adsorbent was determined. The parameters q_m, K_L, K_F, n, and R^2 are presented in Table 4, and the graphical

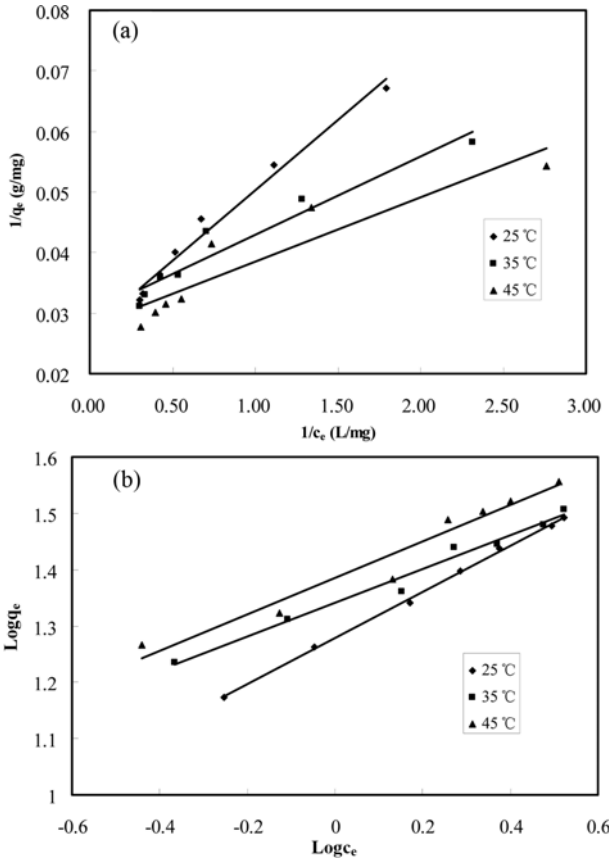

Fig. 8. Langmuir (a) and Freundlich (b) isotherms for the adsorption of Cu(II) on Cu(II)-IIP at 25 °C.

presentations for Langmuir and Freundlich adsorption isotherm are in Fig. 8. The applicability of the isotherm equation to describe the adsorption process was judged by the correlation coefficients of isotherms (r^2). As shown in Table 4, the Cu(II) ions adsorption data fitted the Langmuir and Freundlich equations equally well with correlation coefficients close to unity; however, the Freundlich equation gave a better fit. Different from the Langmuir isotherm model, the Freundlich isotherm model does not predict a maximum metal removal, so that the precipitation occurs following the ligand exchange phase, and results in a continuous steady increase in adsorption, so the data are better fitted to the Freundlich equation.

For the Freundlich model, the slope 1/n is the sorptive intensity; values of n>1 indicate that bonding energies decrease with the increasing surface adsorption densities in accordance with preferential adsorption, occupying surface sites in the order from strongest to weakest binding strength. In addition, n>2 is sometimes interpreted as an indication of an adsorbent with good adsorbent char-

Table 4. Langmuir and Freundlich isotherm constants and correlation coefficients (R^2)

Temperature (°C)	Langmuir isotherm			Freundlich isotherm		
	q_m (mg/g)	K_L (L/mg)	R^2	n	K_F [$mg^{(1-1/n)} \cdot L^{1/n}/g$]	R^2
25	31.95	1.343	0.9816	2.440	18.99	0.9986
35	33.22	2.334	0.9358	3.320	21.92	0.9805
45	35.84	2.632	0.8545	3.085	24.24	0.9523

Table 5. Distribution coefficient and selectivity coefficient data

Adsorb material	K_d (L/g)		κ	K_d (L/g)		κ
	Cu(II)	Pb(II)		Cu(II)	Cd(II)	
Non-IIP	0.428	0.143	2.993	0.481	0.176	2.733
Cu(II)-IIP	2.636	0.0336	78.45	2.333	0.0283	82.44

acteristics for the solute being considered.

7. Selective Adsorption

Competitive adsorption of Cu(II)/Pb(II) and Cu(II)/Cd(II) from their mixtures was also studied in a batch system. K_d and k values are shown in Table 5. The k values of the Cu(II)-IIP sorbent for Cu(II)/Pb(II) and Cu(II)/Cd(II) were 78.45 and 82.44, but the non-IIP sorbent were only 2.993 and 2.733. These results showed that the k values of the Cu(II)-IIP sorbent for Cu(II)/Pb(II) and Cu(II)/Cd(II) were 26.20 and 30.16 times greater than of the non-IIP sorbent, respectively, and the binding ability of the Cu(II)-IIP sorbent for Cu(II) was far stronger than that for Pb(II) and Cd(II). The main reason for the smaller combination ability of Cu(II)-IIP on the Pb(II) and Cd(II) was a template ion Cu(II) imprinting cavity, which was not suited to Pb(II) and Cd(II) in size, shape and spatial arrangement of action sites. The imprinting cavity for Cu(II) had good recognition memory capacity and high combined selectively.

8. Regeneration

Regeneration of any exhausted sorbent is an important issue from both economical and practical viewpoints. The purpose of regeneration is the repeated use of the sorbent material and decreasing cost. The adsorption capacity of Cu(II) on Cu(II)-IIP after ten adsorption/desorption cycles was found to about 86% of the fresh sorbent. The data showed that Cu(II)-IIP had good regeneration capacity for Cu(II).

CONCLUSIONS

A new type of organic-inorganic hybrid Cu(II)-imprinted polymer was successfully prepared with the surface ion imprinting concept with sol-gel process. Thus prepared ion-imprinted polymer exhibited several special characteristics: mild imprinting reactive condition, fine configuration, high adsorption, proper static adsorption capacity, satisfactory selectivity towards Cu(II), and low cost. The thermodynamic parameter showed that the adsorption process was spontaneous and feasible. The Cu(II) ions adsorption data fitted the Langmuir and Freundlich equations equally well with correlation coefficients close to unity, where the Freundlich equation gave a better fit. The kinetic data showed that pseudo-second-order kinetic model agrees very well with the dynamic behavior for the sorption of Cu(II) onto Cu(II)-IIP. This composite sorbent can be potentially used as the solid-phase extraction sorbent for the selective pre-concentration, separation and determination trace Cu(II) in environmental samples.

ACKNOWLEDGEMENTS

This work is supported by the Natural Science Foundation of China (51174096), Industrial Support Project of Huai'an of Jiangsu Province (HAG2010011) and Research Subject of Environmental Protection Department of Jiangsu Province (2013031).

REFERENCES

1. A. Celik and A. Demirbaş, *Energy Sources*, **27**, 1167 (2005).
2. A. Demirbas, *Energy Edu. Sci. Technol.*, **5**, 21 (2000).
3. A. Özer and H. Pirincci, *J. Hazard. Mater.*, **137**, 849 (2006).
4. J. Wang and C. Chen, *Biotechnol. Adv.*, **27**, 195 (2009).
5. B. Zhu, T. Fan and D. Zhang, *J. Hazard. Mater.*, **153**, 300 (2008).
6. A. K. Meena, K. Kadirvelu, G. Mishra, C. Rajagopal and P. Nagar, *J. Hazard. Mater.*, **150**, 604 (2008).
7. J. Shah, M. R. Jan, M. Sadia and H. Atta-ul-Haq, *Korean J. Chem. Eng.*, **30**, 706 (2013).
8. H. Kalavathy, M. I. Regupathi, M. G. Pillai and L. R. Miranda, *Colloids Surf., B: Biointerfaces*, **70**, 35 (2009).
9. O. Amuda, A. A. Giwa and I. Bello, *Biochem. Eng. J.*, **36**, 174 (2007).
10. Y. L. Kang, M. Y. Poon, P. Monash, S. Ibrahim and P. Saravanan, *Korean J. Chem. Eng.*, **30**, 1904 (2013).
11. A. A. Mosa, A. El-Ghamry and P. Trüby, *Water, Air, Soil Pollut.*, **217**, 637 (2011).
12. M. Rashed, *Int. J. Environ. Waste Manage.*, **7**, 175 (2011).
13. A. Mittal, J. Mittal, A. Malviya, D. Kaur and V. Gupta, *J. Colloid Interface Sci.*, **343**, 463 (2010).
14. A. Saeed, M. Sharif and M. Iqbal, *J. Hazard. Mater.*, **179**, 564 (2010).
15. S. Khattri and M. Singh, *J. Hazard. Mater.*, **167**, 1089 (2009).
16. V. K. Gupta, R. Jain, M. Shrivastava and A. Nayak, *J. Chem. Eng. Data*, **55**, 5083 (2010).
17. C. Pang, Y. Liu, X. Cao, R. Hua, C. Wang and C. Li, *J. Radioanal. Nucl. Chem.*, **286**, 185 (2010).
18. Q. Fan, X. Tan, J. Li, X. Wang, W. Wu and G. Montavon, *Environ. Sci. Technol.*, **43**, 5776 (2009).
19. Q. Fan, D. Shao, J. Hu, W. Wu and X. Wang, *Surf. Sci.*, **602**, 778 (2008).
20. L. Chen and X. Gao, *Appl. Radiat. Isot.*, **67**, 1 (2009).
21. Z. Niu, Q. Fan, W. Wang, J. Xu, L. Chen and W. Wu, *Appl. Radiat. Isot.*, **67**, 1582 (2009).
22. S. Wang, D. Yu, Y. Huang and J. Guo, *J. Appl. Polym. Sci.*, **119**, 2065 (2011).
23. G. Dotto and L. Pinto, *Carbohydr. Polym.*, **84**, 231 (2010).
24. X. Y. Huang, X. Y. Mao, H. T. Bu, X. Y. Yu, G. B. Jiang and M. H. Zeng, *Carbohydr. Polym.*, **83**, 528 (2011).
25. S. Kittinaovarat, P. Kansomwan and N. Jiratumnukul, *Appl. Clay Sci.*, **48**, 87 (2010).
26. C. M. Futalan, C. C. Kan, M. L. Dalida, K. J. Hsien, C. Pascua and M. W. Wan, *Carbohydr. Polym.*, **83**, 528 (2011).
27. V. M. Boddu, K. Abburi, J. L. Talbott and E. D. Smith, *Environ. Sci. Technol.*, **37**, 4449 (2003).
28. B. Godlewska-Żyłkiewicz, B. Leœniewska and I. Wawreniuk, *Talanta*, **83**, 596 (2010).
29. T. Prasada Rao, S. Daniel and J. Mary Gladis, *TrAC, Trends Anal. Chem.*, **23**, 28 (2004).
30. M. Saraji and H. Yousefi, *J. Hazard. Mater.*, **167**, 1152 (2009).
31. E. Zambrzycka, D. Roszko, B. Lesniewska, A. Z. Wilczewska and B. Godlewska-Zylkiewicz, *Spectrochim. Acta - Part B A.*, **66**, 508 (2011).
32. J. B. Wu and Y. L. Yi, *Korean J. Chem. Eng.*, **30**, 1111 (2013).
33. A. Kaewchada, C. Borvornpongsakul and A. Jaree, *Korean J. Chem. Eng.*, **29**, 1279 (2012).